

# Electronic property and molecule design for luminescent metal complexes of tris(8-hydroxyquinoline) gallium

SU Zhongmin (苏忠民)<sup>1, 2</sup>, GAO Hongze (高洪泽)<sup>1</sup>, CHENG Hong (程 红)<sup>1</sup>, CHU Bei (初 蓓)<sup>1</sup>, CHEN Lihua (陈丽华)<sup>1</sup>, WANG Rongshun (王荣顺)<sup>1</sup>, WANG Yue (王 悦)<sup>2</sup> & SHEN Jiacong (沈家骢)<sup>2</sup>

1. Institute of Functional Material Chemistry, Department of Chemistry, Northeast Normal University, Changchun 130024, China;

2. Key Laboratory for Supramolecular Structure and Spectroscopy, Institute of Theoretical Chemistry, Jilin University, Changchun 130023, China

Correspondence should be addressed to Su Zhongmin(email: zmsu@nenu.edu.cn)

Received August 14, 2000

**Abstract** By means of *ab initio* HF and DFT B3LYP methods, the structure of Gaq<sub>3</sub> (q = 8-hydroxyquinoline) was optimized. The frontier molecular orbital characteristics and energy levels of Gaq<sub>3</sub> have been analyzed systematically in order to study the electronic transition mechanism in Gaq<sub>3</sub>. Three derivatives of Gaq<sub>3</sub> and their polymers were designed and the possibilities that they were employed as luminescent materials were discussed. The regularities and characteristic of energy bands of Gaq<sub>3</sub> and its derivatives were also investigated. The results show that the electronic  $\pi$ - $\pi^*$  transitions in Gaq<sub>3</sub> are localized on the quinolate ligands. The emission of Gaq<sub>3</sub> is due to the electron transitions from a phenoxide donor to a pyridyl acceptor. Two possible electron transfer pathways are presented, one by carbon atoms, and the other via metal cation Ga<sup>3+</sup>. The derivatives of Gaq<sub>3</sub> may possess high luminescence efficiency.

**Keywords:** tris(8-hydroxyquinoline) gallium, *ab initio*, DFT, electronic property, energy band structure.

The efficient organic electroluminescent devices (OLED), in which tris(8-hydroxyquinoline)-aluminum (Alq<sub>3</sub>) was used as emitting material, were first reported by Tang and VanSlyke<sup>[1]</sup>. The electroluminescent (EL) efficiency of OLEDs has been improved greatly<sup>[2-5]</sup>. Many EL studies based on Alq<sub>3</sub> and other metal chelates have been carried out. In 1994, Burrows<sup>[6]</sup> and coworkers systematically investigated the EL devices based on Gaq<sub>3</sub> and Alq<sub>3</sub>, showing that Gaq<sub>3</sub> has a thin film PL quantum efficiency of only 25% of that for Alq<sub>3</sub>. However, the power efficiency of its light-emitting devices is higher than that of Alq<sub>3</sub> by 50%, suggesting that the Gaq<sub>3</sub> is a superior emitter material for display applications. Wang<sup>[7]</sup> and coworkers first obtained the single crystal structure of Gaq<sub>3</sub> and demonstrated the charge transfer mechanism of Gaq<sub>3</sub>. The luminescence mechanisms of metal organic compounds are quite complicated<sup>[8-12]</sup> and there are few qualitative or quantitative systematic explanations for the metal chelate luminescence process<sup>[13]</sup>. We first optimized the geometry of Gaq<sub>3</sub> by *ab initio* HF and DFT B3LYP methods, and analyzed the electronic properties and composition characteristics of molecular orbitals. The excited state calculation was carried out using single-excitation. In order to develop efficient EL materials, which

possess both small molecule and polymer properties, three derivatives of Gaq<sub>3</sub> were designed and the effects of substituent on its properties are discussed. The energy bands of three derivatives were calculated using semi-experience EHMO-CO methods.

## 1 Calculation methods and models

All the results presented in this paper were obtained at the *ab initio* HF and DFT B3LYP levels by means of GAUSSIAN 94 program<sup>[14]</sup>. The calculation model of Gaq<sub>3</sub> is shown in fig. 1. In order to save calculation time, the C<sub>3</sub> symmetry was kept in the course of calculation. We have fully optimized the structures of the complexes using sequence of basis sets of increasing flexibility including the minimal STO-3G, the split-valence 3-21G, both 6-31G and effective core potentials (ECPs) and valence-double Zeta LANL2DZ basis sets, analyzed the composition characteristics of molecular orbitals, and carried out calculation of excited states using single-excitation. We also optimized the structures and molecular characteristics of three derivants of Gaq<sub>3</sub> using HF/6-31G level theory and took into account the effects of substituent on them. The regularity and characteristics of energy bands of three derivants were investigated for providing the basis for further molecular design of conductive and luminescent functional materials and device using semi-experience EHMO-CO methods<sup>[15]</sup>, in which the optimized geometries at the HF/6-31G level of theory were used. All the calculations were performed on the SGI Origin 200 server.

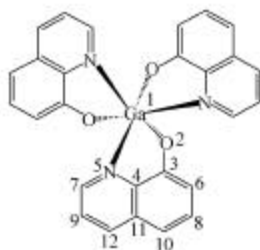


Fig. 1. Calculation model of Gaq<sub>3</sub>.

## 2 Calculation results and discussion

### 2.1 Stable geometrical structure of Gaq<sub>3</sub>

The optimized geometry parameters are shown in table 1. The atom numbering scheme is presented in fig. 1.

The calculation results obtained by methods of HF and B3LYP are approximate to each other and are also close to the experimental values<sup>[7]</sup>. The bond lengths obtained at the B3LYP/6-31G level are extremely identical to the experimental ones and the maximum error is 0.000 3 nm lower. The maximum error of the calculation results is about 0.005 nm. The errors of the calculation at the HF/STO-3G and HF/LANL3DZ levels are bigger compared with the calculated results at the HF/6-31G and B3LYP/6-31G levels. But the other basis sets have given well-calculated geomet-

Table 1 The geometries optimized by different methods and basis sets

Bond length /nm	HF			B3LYP 6-31G	Exp. <sup>[7]</sup>	Bond angle/(°)	HF			B3LYP 6-31G	Exp. <sup>[7]</sup>
	STO-3G	LANL2DZ	6-31G				STO-3G	LANL2DZ	6-31G		
R(1,2)	0.188 6	0.185 0	0.189 3	0.193 3	0.193 7	A(1,2,3)	119.81	121.26	118.95	115.99	115.04
R(2,3)	0.132 5	0.132 9	0.132 0	0.133 0	0.131 7	A(3,4,5)	115.37	115.50	115.37	115.23	115.61
R(3,4)	0.142 8	0.143 0	0.142 4	0.143 6	0.141 7	A(1,5,4)	108.85	107.33	109.35	109.85	109.57
R(4,5)	0.135 8	0.137 0	0.136 3	0.137 1	0.137 4	A(4,3,6)	117.56	118.06	117.79	117.43	117.10
R(1,5)	0.218 7	0.222 7	0.214 2	0.210 8	0.211 2	A(4,5,7)	119.67	119.72	119.68	119.40	119.06
R(3,6)	0.137 4	0.137 7	0.137 2	0.139 6	0.139 2	A(3,6,8)	120.23	120.08	120.23	120.37	120.41
R(5,7)	0.130 2	0.131 2	0.130 8	0.133 5	0.133 2	A(5,7,9)	121.37	121.82	121.90	121.77	121.03
R(6,8)	0.141 5	0.141 8	0.140 9	0.141 1	0.142 2	A(6,8,10)	122.47	122.25	121.37	122.55	121.51
R(7,9)	0.142 3	0.141 9	0.140 8	0.141 1	0.140 4	A(7,9,12)	119.32	119.30	119.33	119.61	119.31
R(8,10)	0.138 7	0.137 6	0.136 9	0.139 0	0.134 0	A(8,10,11)	119.02	119.04	118.98	119.13	120.83
R(4,11)	0.141 2	0.140 6	0.140 2	0.142 8	0.141 5	A(9,12,11)	120.35	119.98	120.03	120.22	119.03
R(9,12)	0.137 5	0.137 2	0.136 5	0.138 4	0.143 0	A(4,11,10)	118.52	118.60	118.49	118.31	117.70
R(10,11)	0.142 1	0.142 0	0.141 4	0.141 7	0.142 2	A(4,11,12)	116.38	116.59	116.49	116.31	117.60
R(11,12)	0.141 5	0.142 3	0.141 7	0.142 2	0.140 2	A(10,11,12)	124.98	124.79	125.00	125.36	124.70

Exp.: crystal data.

rical structure. Although the calculation error is bigger at the HF/LANL2DZ level, it does not exceed 6%. Compared with some researches<sup>[16]</sup>, the geometry optimized at the STO-3G and 6-31G levels is more precise than that of semi-experience CNDO/2, INDO and MNDO methods. At the same time, the errors of several methods are very small in calculated bond angle. The biggest error is lower than 7%, especially the values used DFT(B3LYP) methods are more close to the experimental ones. The coordinations between gallium and the nitrogen and oxygen atoms in 8-hydroxyquinoline form three distorted pentagon structures and three 8-hydroxyquinoline ligand plans have been wrested, which results in C8 and C9 direct toward outside, and C10 and C12 draw back to inside. Compared with the free 8-hydroxyquinoline, the bond lengths of C3-C4, C4-C5, C3-C6, N5-C7, C7-C9, C8-C10, C11-C12 become shorter, while those of C6-C8, C9-C12, C10-C11 become longer. The experimental bond lengths of Ga-O and Ga-N are 0.193 7 and 0.211 2 nm, respectively, while the calculation values at the HF/6-31G and B3LYP/6-31G levels are 0.198 3, 0.193 3 and 0.214 2, 0.210 8 nm, respectively. The error is only 0.000 4 nm. The DFT method at the 6-31G level basis set has reflected well the geometry structure of this kind of metal coordination complex. The reason that better results were obtained when B3LYP/6-1G methods are used is that it allows for configuration interaction. So the result even approaches the fact.

## 2.2 Analysis of Gaq<sub>3</sub> molecular orbital population

For metal chelate, the structure of the ground state and excited state, electron transition and the energy transfer mechanism and so on have pronounced effect on its EL efficiency. In order to explore the electron transition property of Gaq<sub>3</sub>, we made a systematic analysis on the population of Gaq<sub>3</sub> molecular orbit. It was based on the stable geometrical structure optimized at the *ab initio* HF/6-31G and DFT B3LYP/6-31G levels. Meanwhile, the square sum of all kinds of atoms or molecular parts in Gaq<sub>3</sub> indicates the contribution of each atom or molecular moiety to one molecular orbit. All the atoms in Gaq<sub>3</sub> were divided into five parts: ( i ) phenol ring C(I), including

atoms with numbers of 2, 3, 4, 6, 8, 10 and 11; (ii) pyridine ring C(II), including atoms with numbers of 4, 5, 7, 9, 11 and 12; (iii) all oxygen atoms; (iv) all nitrogen atoms; (v) gallium atom. 20 orbits are extracted from the frontier occupied orbits and unoccupied orbits, respectively. The results are summarized in tables 2 and 3.

Table 2 The molecular orbital components of Gaq<sub>3</sub> computed at the HF/6-31G level

MO	Orbital symm.	Orbital energy/eV	Ga	C(I)	C(II)	O	N
148	E	7.612 7	3.7	18.2	81.6	0.5	5.3
147	A	7.559 9	5.1	30.6	65.7	1.2	0.4
146	E	7.404 8	1.9	26.9	75.9	0.9	5.2
145	E	7.404 8	1.9	26.9	75.9	0.9	5.2
144	A	7.396 7	0.2	33.9	71.1	1.0	4.4
143	E	7.199 9	0.7	73.0	29.4	0.1	0.9
142	E	7.199 9	0.7	73.0	29.5	0.1	0.9
141	A	6.870 1	6.4	71.4	24.9	0.9	5.6
140	E	6.323 7	0.3	20.2	83.7	0.1	1.1
139	E	6.323 7	0.3	20.2	83.7	0.1	1.1
138	A	6.082 1	6.1	9.6	89.1	0.7	3.0
137	E	5.231 2	0.2	81.2	35.1	4.0	6.4
136	E	5.231 2	0.2	81.1	35.0	4.0	6.4
135	A	5.090 2	0.3	82.8	33.3	3.4	6.5
134	E	3.288 5	0.1	61.8	75.7	0.0	0.3
133	E	3.288 5	0.1	61.8	75.8	0.0	0.3
132	A	2.956 3	0.3	58.5	77.1	0.0	0.9
131	A	1.906 4	0.8	24.0	81.0	2.4	24.7
130	E	1.809 3	0.3	24.3	81.0	1.6	24.1
129(LUMO)	E	1.809 3	0.3	24.4	80.9	1.6	24.1
128(HOMO)	A	-7.376 0	1.1	84.3	21.6	22.7	4.9
127	E	-7.402 6	0.6	87.5	20.9	21.5	4.9
126	E	-7.402 6	0.6	87.5	21.0	21.5	4.8
125	E	-9.181 2	0.0	75.3	63.1	0.3	0.1
124	E	-9.181 2	0.0	75.4	63.1	0.3	0.1
123	A	-9.276 7	0.0	76.2	62.4	0.1	0.1
122	E	-10.908 3	0.4	41.9	66.6	24.6	17.1
121	E	-10.908 3	0.4	41.9	66.6	24.5	17.1
120	A	-11.121 1	0.4	35.7	70.8	19.7	15.5
119	A	-11.204 6	3.5	82.0	30.2	48.5	9.7
118	A	-11.204 6	3.3	82.2	30.3	48.6	9.7
117	A	-11.710 2	6.1	85.5	26.4	46.7	5.6
116	A	-12.390 8	1.6	71.1	45.6	20.7	15.3
115	E	-12.409 9	1.6	45.3	72.4	9.3	37.0
114	E	-12.409 9	1.6	45.3	72.5	9.3	37.0
113	E	-12.672 7	0.9	64.8	54.8	13.2	19.6
112	E	-12.672 7	0.8	64.9	54.7	13.2	19.5
111	A	-13.250 7	2.5	57.0	61.8	6.3	18.9
110	E	-13.839 8	0.6	73.9	29.1	37.9	8.1
109	E	-13.839 8	0.7	73.8	29.0	37.9	8.1

Table 3 The molecular orbital components of Gaq<sub>3</sub> computed at the B3LYP/6-31G level

MO	Orbital symm.	Orbital energy/eV	Ga	C(I)	C(II)	O	N
148	A	3.550 3	4.0	21.6	75.9	1.5	0.6
147	A	3.524 2	7.9	61.5	33.9	4.0	3.2
146	E	3.193 8	0.3	78.5	23.5	0.4	1.5
145	E	3.192 7	0.3	78.5	23.5	0.4	1.5
144	A	2.696 1	6.2	56.1	40.5	3.0	5.9
143	E	2.483 6	0.3	16.7	85.6	0.1	0.9
142	E	2.483 3	0.3	16.7	85.7	0.1	0.9
141	A	2.3405	0.2	40.2	67.1	1.4	5.3
140	A	2.340 2	0.2	40.2	67.0	1.4	5.3
139	A	2.336 4	2.7	40.8	64.2	1.4	6.2
138	A	2.047 7	13.7	14.4	77.2	4.0	10.1
137	E	0.954 0	0.3	85.5	30.6	5.9	6.5
136	E	0.953 8	0.3	85.4	30.4	5.9	6.5
135	A	0.857 4	0.4	86.5	29.9	5.1	6.4
134	E	-0.483 8	0.1	58.5	75.4	0.0	0.1
133	E	-0.484 6	0.1	58.4	75.4	0.0	0.1
132	A	-0.684 4	0.1	56.1	76.0	0.1	0.5
131	A	-1.743 2	0.8	24.5	82.4	3.8	26.9
130	E	-1.825 6	0.4	24.4	82.5	2.3	25.9
129(LUMO)	E	-1.826 2	0.4	24.4	82.6	2.3	25.9
128(HOMO)	A	-5.176 5	1.9	85.5	21.1	31.4	2.8
127	E	-5.189 8	1.2	89.2	20.0	30.9	3.2
126	E	-5.190 1	1.2	89.2	20.0	30.9	3.2
125	E	-6.950 1	4.4	85.6	28.1	47.9	7.5
124	E	-6.951 7	4.7	85.2	28.0	47.7	7.5
123	E	-7.024 9	0.2	75.3	55.5	2.7	0.3
122	E	-7.025 5	0.2	75.2	55.5	2.6	0.3
121	A	-7.091 6	0.0	75.5	55.8	0.3	0.1
120	A	-7.521 3	10.7	81.6	25.1	42.9	4.3
119	E	-7.839 1	0.8	49.6	55.6	26.9	14.3
118	E	-7.839 9	0.8	49.7	55.8	26.9	14.4
117	A	-7.981 2	1.1	50.5	54.2	27.7	12.0
116	E	-8.496 0	3.8	39.7	75.4	7.8	39.7
115	E	-8.496 5	3.9	39.8	75.4	7.8	39.7
114	A	-8.964 9	1.7	54.8	63.6	10.6	19.5
113	E	-9.171 4	0.5	58.9	61.5	11.5	17.6
112	E	-9.172 5	0.6	59.0	61.4	11.5	17.5
111	A	-9.444 9	5.5	57.6	57.7	5.9	13.9
110	E	-9.823 4	0.3	71.7	36.3	10.4	7.2
109	E	-9.823 4	0.3	71.7	36.2	10.4	7.2

The result analysis demonstrates that the orbital populations coincide for the two methods, which implies that the molecular theoretical results are reliable. The electron clouds of HOMO, HOMO<sub>-1</sub>, and HOMO<sub>-2</sub> are concentrated on the carbon and oxygen of phenol ring in 8-hydroxy-quinoline ring ligand. The electronic cloud is mainly composed of the p-orbital ingredient and includes oxygen of 20%—30%, nitrogen of 3%—5%, and few s orbital characters are observed. While the electronic clouds of LUMO, LUMO<sub>+1</sub> and LUMO<sub>+2</sub> are concentrated on the pyridine

ring in 8-hydroxyquinoline ring, which is mostly composed of the  $p\text{-}\pi^*$  orbits of carbon and nitrogen, s orbit is very little too, including nitrogen occupying 2%—4%. Gallium ingredient is still very little, occupying 0.3%—2%, which only contributes little in deeper orbit. Other orbits appear as the form of un-bond. Fig. 2 clearly exhibits the feature of the frontier orbit.

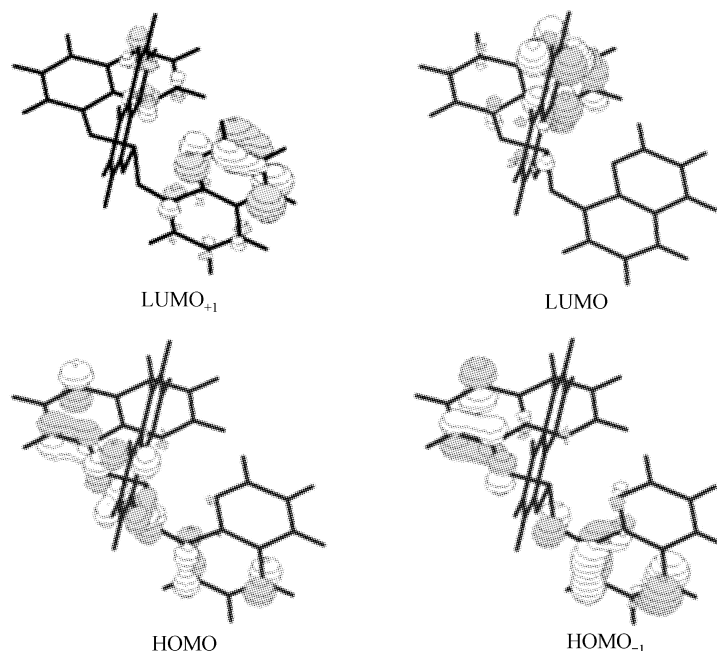


Fig. 2. Shapes of selected MOs of  $Gq_3$ .

In order to obtain better understanding of the contribution of gallium to molecular stability and the electron excitation transition, d and p polarization functions are introduced, respectively. Meanwhile we apply B3LYP/6-31G\*\* method to making further molecular orbitals analysis. The result is shown in table 4. There are 10 orbits extracted in occupied and unoccupied orbits. To make more clear, the d orbits of gallium are listed alone.

The analysis demonstrates that the form of MO and the distributed feature have little change after Ga is introduced to the d orbit basis set. After d orbits of Ga are considered, the contribution of Ga to HOMO and  $HOMO_{-1}$  has little increase, but that of the ligands is dominant. So the difference between optical luminescence and electrical luminescence in  $Alq_3$  does not originate from the participation of d orbit of Ga, while the structure change for the difference of metallic radius may be the key. The bond lengths calculated for Al-O and Al-N in  $Alq_3$  are 0.108 90 and 0.212 4 nm<sup>[17]</sup> respectively. Every 8-hydroxyquinoline part is very near in  $Alq_3$ . So it is important for the electron to transfer in the molecule. For  $Gaq_3$ , three-leaf molecular parts separate and two molecules form crystal through ligand, and it may be possible that electron transfers between molecular parts in two molecules.

The experiment indicates that the UV maximum absorption of  $Gaq_3$  is 393.4 nm. Meanwhile

Table 4 The molecular orbital components of Gaq<sub>3</sub> computed at the B3LYP/6-31G\*\* level

MO	Orbital symm.	Orbital energy/eV	Ga	Ga(d)	C(I)	C(II)	O	N
138	E	5.902 2	61.7	5.7	5.9	34.2	2.1	5.6
137	E	5.193 3	0.6	0.3	85.4	30.3	5.8	6.0
136	E	5.193 3	0.5	0.2	85.4	30.4	5.8	6.0
135	A	5.046 4	1.3	0.9	86.0	29.4	4.6	5.4
134	E	3.225 1	0.6	0.3	58.9	73.7	0.0	0.6
133	E	3.225 1	0.7	0.4	58.8	73.7	0.0	0.6
132	A	2.896 1	0.5	0.2	56.4	74.5	0.0	1.3
131	A	1.815 3	1.6	0.1	25.3	81.0	3.7	25.8
130 (LUMO <sub>+1</sub> )	E	1.723 3	0.6	0.3	25.0	81.9	2.0	24.6
129 (LUMO)	E	1.723 3	0.7	0.3	25.0	81.7	2.0	24.6
128 (HOMO)	A	-7.226 0	5.1	0.5	83.2	20.1	28.5	2.9
127 (HOMO <sub>-1</sub> )	E	-7.237 7	2.3	0.5	87.4	20.1	28.7	3.1
126	E	-7.237 7	2.1	0.6	87.9	20.1	28.8	3.1
125	E	-8.949 9	0.2	0.1	73.4	58.2	0.9	0.4
124	E	-8.949 9	0.2	0.1	73.6	58.1	1.0	0.4
123	A	-9.240 4	0.1	0.1	74.4	57.3	0.2	0.5
122	E	-10.769 3	6.6	3.2	81.4	26.5	54.5	8.7
121	E	-10.769 3	6.0	2.6	81.7	26.9	54.6	8.9
120	A	-10.951 9	28.2	3.2	62.3	18.7	42.2	6.0
109	E	-11.221 8	0.9	0.3	48.1	56.6	27.4	14.8

there are a series of strong absorption at around 335 nm. The calculation of single-excited configuration interaction in *ab initio* shows that the first excited state is mainly attributed to electron excitation from the highest occupied orbit to the lowest unoccupied orbit, namely the transition results of HOMO→LUMO, HOMO→LUMO<sub>+1</sub>, HOMO→LUMO<sub>+2</sub> and HOMO<sub>-1</sub>→LUMO<sub>+1</sub>. The other strong absorption results from the electron transition from the highest occupied orbits to the even higher unoccupied orbits, which is formed by HOMO→LUMO<sub>+3</sub>, together with other orbital transitions. According to the analysis of molecular orbital ingredient, we found that when the electron transition is from the ground state to the excited state, the electron transfers from phenol ring with oxygen to pyridine ring with nitrogen. In the ground state, oxygen orbital population is about 20%, but it decreases to 2% in excited state. While that of nitrogen increases from 3% to 25%. Oxygen is the electron donor, and nitrogen is the electron acceptor. The electron that transfers in 8-hydroxyquinoline ligand causes the electroluminescence. There are two ways of electron transfer: one is the direct transition through carbon in quinoline ring; other is through the metal ion, which is not only a support but also a bridge of electron transfer. The special molecular packing can lead to the interaction of two adjacent molecules, to be found clearly in the crystal structure. It is possible for the  $\pi$ - $\pi$  interactions to provide the passage for electron transfer among molecules.

The luminescence of metallic complex material in electroluminescence devices is due to the combination of electron and hole. The electron injected from cathode should fill in the pyridine ring, which has become the electron potential energy container. While the hole injected from the anode should concentrate on the phenol ring, which has become the hole potential energy con-

tainer. Because the energy of unoccupied orbit is positive, the electron filling up the pyridine ring is not stable, which will transit to phenol one. The combination of electron and hole at two energy levels will result in luminescence. In  $\text{GaQ}_3$  molecule, Ga makes the ligands have a certain space, which leads possibly to the interaction of phenol and pyridine between two molecules in solid. The intensity of electroluminescence in  $\text{GaQ}_3$  is stronger than that in  $\text{AlQ}_3$ , but the metal ion  $\text{Ga}^{3+}$  contributes less to luminescence directly.

### 2.3 Analysis of electronic property and molecular orbital population in $\text{GaQ}_3$ derivative

The above analysis shows that the ligands can determine the spectral property of  $\text{GaQ}_3$ . Different substitute groups will have different effects on the electron property of  $\text{GaQ}_3$ . If the distribution and orbital energy level of nitrogen and oxygen change, the spectral property will change too. The organic styrene derivative compounds have shown clearly superiority in conduction, optical and nonlinear optical properties<sup>[18–22]</sup> and so on. Just for it, we designed three kinds of  $\text{GaQ}_3$  derivatives (fig. 3). For two derivatives, two hydrogens, H8 and H9, are substituted by the styryl and ethylene (fig. 3, **1** and **2**). For the third derivative, the H10 is replaced by cyano, but it still keeps  $\text{C}_3$  symmetry (fig. 3, **3**). We have obtained the stable geometric-optimized structures of three derivatives by using HF/6-31G methods.

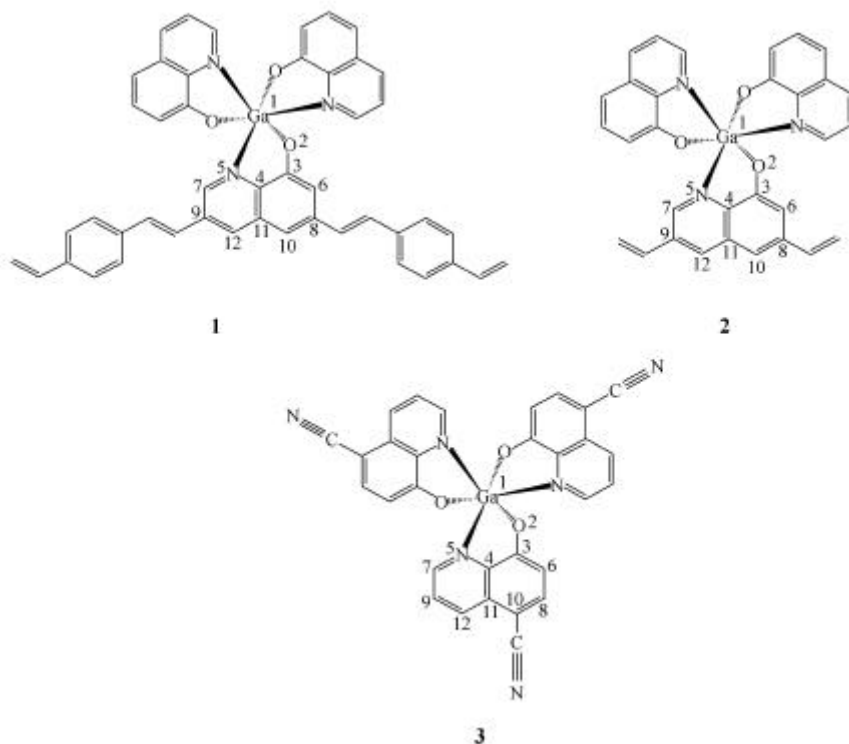


Fig. 3. The calculation models of  $\text{GaQ}_3$ 's derivatives.

**2.3.1 Energy level distribution of three derivatives.** The molecular orbit energy of  $\text{GaQ}_3$  and its derivatives is shown in table 5. There are 10 orbits extracted from the occupied and 10 from unoc-



cupied molecular orbits.

Table 5 Orbital energy of Gaq<sub>3</sub>'s derivatives/eV

1		2		3		Gaq <sub>3</sub>	
Virt.	Occ.	Virt.	Occ.	Virt.	Occ.	Virt.	Occ.
4.049 4	−7.069 6 <sub>(HOMO)</sub>	5.229 8	−7.411 1 <sub>(HOMO)</sub>	2.970 1	−8.603 8 <sub>(HOMO)</sub>	6.082 1	−7.376 0 <sub>(HOMO)</sub>
3.675 5	−7.404 0	5.105 4	−7.465 0	2.280 6	−8.642 9	5.231 2	−7.402 6
3.385 4	−7.478 0	5.039 9	−7.490 8	2.280 6	−8.642 9	5.231 2	−7.402 6
3.328 5	−7.501 4	4.111 9	−8.258 2	2.156 5	−10.317 3	5.090 2	−9.181 2
3.203 9	−7.982 5	3.336 1	−9.122 1	2.058 3	−10.317 3	3.288 5	−9.181 2
2.666 2	−8.888 7	3.229 2	−9.153 2	2.058 3	−10.354 6	3.288 5	−9.276 7
2.002 2	−9.127 0	2.395 4	−9.552 1	1.974 5	−10.885 2	2.956 3	−10.908 3
1.958 7	−9.147 2	2.006 0	−10.872 1	0.690 9	−10.885 2	1.906 4	−10.908 3
1.881 7	−9.163 8	1.971 5	−10.903 4	0.646 8	−10.887 4	1.809 3	−11.121 1
1.619 9 <sub>(LUMO)</sub>	−9.562 7	1.912 4 <sub>(LUMO)</sub>	−10.975 3	0.646 8 <sub>(LUMO)</sub>	−11.363 3	1.809 3 <sub>(LUMO)</sub>	−11.204 6

Occ.:occupied orbits; Virt.:unoccupied orbits.

The calculation results indicate that the interaction between p-styrene and frontier molecular orbit of quinoline is obvious, which leads to the increase of  $\pi$ -electron conjugate effect. For the cyano-substituted derivative, the HOMO and LUMO energy levels go down at the same time, but the energy gap is 9.323 5 eV, which is much larger than that of unsubstituted Gaq<sub>3</sub>, suggesting that it is possible to prepare new luminescent materials with different emitting colors by the substitut- ing reactions and improve the performance of devices through different substitute groups.

2.3.2 Analysis of molecular orbital ingredient in three derivatives. We divided molecular or- bital ingredients into several parts as follows: (a) Ga, (b) unsubstituted phenol ring, (c) unsubsti- tuted pyridine ring, (d) substituted phenol ring, (e) substituted pyridine ring, (f) substituted group with phenol ring, (g) substituted group with pyridine ring. The calculation results of derivatives **1** and **2** are presented in tables 6 and 7.

Table 6 The molecular orbital components of Gaq<sub>3</sub>'s derivative **1** (%)

Orbitals	a	b	c	d	e	f	g
206	0.0	0.0	0.1	1.9	1.5	95.3	1.7
205	0.0	0.1	0.1	2.8	2.4	1.7	94.7
204	0.0	4.5	5.3	18.5	25.7	19.8	38.6
203	0.1	35.1	42.4	0.7	0.8	0.3	0.5
202	0.1	22.8	27.5	2.0	2.8	2.0	2.3
201	0.3	0.3	0.7	9.2	31.3	37.9	24.3
200	0.7	18.6	66.6	0.8	1.1	0.9	0.1
199	0.5	3.9	12.4	0.9	1.5	0.6	0.5
198	0.2	0.5	1.3	21.0	41.4	31.8	8.1
197(LUMO)	0.2	0.1	0.3	16.4	37.7	0.1	51.9
196(HOMO)	0.1	0.0	0.2	37.8	15.0	53.1	0.7
195	0.3	6.9	2.0	28.5	13.0	10.6	30.1
194	0.5	66.2	15.3	5.2	2.4	1.8	6.0
193	0.5	13.7	3.3	2.0	1.1	0.7	1.7
192	0.2	0.2	0.3	34.8	9.7	17.3	42.8
191	0.0	0.1	0.1	36.6	25.5	36.8	17.0
190	0.0	60.6	50.6	0.0	0.1	0.0	0.0
189	0.0	0.0	0.0	0.1	0.1	99.5	0.0
188	0.0	15.9	13.0	0.1	0.1	0.4	0.0
187	0.0	0.0	0.0	0.0	0.1	0.1	99.8

Table 7 The molecular orbital components of Gaq<sub>3</sub>'s derivative **2** (%)

Orbitals	a	b	C	d	e	f	g
152	0.3	1.9	2.0	65.9	27.7	0.2	18.8
151	0.1	49.0	16.9	0.2	1.0	0.0	0.3
150	0.2	33.0	11.9	4.0	2.6	0.0	1.5
149	0.3	0.5	1.3	24.3	23.7	30.0	26.1
148	0.1	34.8	42.0	0.3	0.5	0.0	0.0
147	0.1	27.2	32.6	0.7	0.9	0.1	0.3
146	0.1	0.4	0.8	40.2	52.7	9.6	19.7
145	0.7	15.7	56.3	1.2	3.0	0.0	0.4
144	0.5	6.5	21.9	0.7	1.1	0.0	0.2
143(LUMO)	0.5	0.7	2.4	20.9	71.2	1.7	4.4
142(HOMO)	0.5	5.5	1.9	69.4	18.6	3.2	1.4
141	0.6	46.8	10.8	9.6	2.9	0.7	0.1
140	0.6	34.1	8.0	0.8	0.5	0.0	0.0
139	0.0	0.1	0.1	52.5	38.2	21.9	8.9
138	0.0	51.6	43.1	0.0	0.1	0.0	0.0
137	0.0	24.9	20.5	0.1	0.1	0.1	0.0
136	0.2	0.4	0.4	26.2	28.0	16.6	33.1
135	0.1	1.4	2.2	25.3	41.2	29.0	5.5
134	0.3	21.0	44.6	3.5	4.8	4.3	0.7
133	0.3	11.0	27.2	3.0	2.2	1.1	0.7

It can be seen in table 6 that the  $\pi$ ,  $\pi^*$  molecular orbit feature of styryl is reflected in the frontier molecular orbits. In the HOMO of **1**, the styryl occupies 54%, which just shows an efficient combination with the quinoline ring. In HOMO, the phenol ring of quinoline and the styryl are the main ingredients, while the pyridine and joined styryl are the main composition in LUMO. It not only maintains the MO distribution feature of the original Gaq<sub>3</sub> but also induces the character of styryl. The electronic cloud distribution of LUMO<sub>-1</sub>, LUMO<sub>-2</sub>, HOMO<sub>+1</sub> and HOMO<sub>+2</sub> is similar to Gaq<sub>3</sub>. In conclusion, if it is approximate to Gaq<sub>3</sub> in energy gap and orbital distribution, it may be a luminescent material. But the styryl leads to the increase of electron transfer ability and some electronic and optical properties of styryl are introduced. **1** is the combination of Gaq<sub>3</sub> and styryl, which can be used as efficient luminescent material.

The results in table 7 suggest that for derivative **2** the electron cloud in the frontier-occupied molecular orbit has no clear change compared with Gaq<sub>3</sub>. From table 7 we can conclude that there is the ethylene orbital feature, which appears in deep MO of 139, 136 and 135. So it should affect the higher energy luminescence spectrum. The optical property of complex is near that of Gaq<sub>3</sub> in the energy gap and orbital distribution. There is less change in the rule of electron transition and the optical characteristics.

The form of the frontier molecular orbit in derivative **3** is lined in table 8. It is divided as (a) Ga, (b) phenol ring, (c) pyridine ring, (d) three cyanogens. It can be seen that electron cloud distribution of nitrogen and oxygen decreases compared with that of Gaq<sub>3</sub>. Though its electron distribution is less than that of the styryl in derivative **1**, it is important that the substituted group provides mainly ingredient in deep orbit (137—140). The electronic property will be affected by

the cyanogen substituted on the base of original Gaq<sub>3</sub>. The increase of Eg in **3** will lead to the blue-shift of emission, and we can obtain good blue-luminescent material.

Table 8 The molecular orbital components of Gaq<sub>3</sub>'s derivative **3** (%)

Orbitals	a	b	c	3CN
156	0.8	56.4	36.6	32.9
155	0.1	67.2	68.1	1.4
154	0.1	67.2	68.0	1.4
153	0.2	64.8	56.7	7.1
152	0.1	30.7	60.1	27.3
151	0.1	30.7	60.1	27.3
150	0.1	34.2	72.9	18.8
149	0.8	41.1	53.1	9.0
148(LUMO)	0.5	39.9	54.1	8.6
147(HOMO)	0.6	39.9	54.0	8.6
146	0.4	70.5	16.5	17.6
145	0.4	70.9	15.6	18.7
144	0.4	70.8	15.6	18.7
143	0.0	74.9	63.4	0.8
142	0.0	74.9	63.4	0.8
141	0.0	75.0	61.2	2.0
140	0.0	16.4	9.8	79.5
139	0.0	16.4	9.7	79.6
138	0.0	17.4	10.5	78.4
137	0.2	23.4	20.1	65.4

**2.3.3 Energy gap structure of the polymer in Gaq<sub>3</sub> derivatives.** The experiments show that PPV possess good conduction and luminescence function. In order to obtain the materials that are combination of PPV and metal complex, we designed one-dimension polymer system with the duplicate units formed by two quinoline rings in two Gaq<sub>3</sub> and high-polymer-embedded systems of corresponding p-styryl and ethylene derivative, which were marked by p-Gaq<sub>3</sub>, p-1 and p-2. We calculated the energy gap structure of these polymers by using semi-experience EHMO-CO method in quantum chemistry, and the results are shown in fig. 4.

According to the solid energy gap theory, the electric conductivity is

$$S = enu,$$

where  $e$  is the charge-loaded current,  $n$  the density per volume,  $u$  the transmit velocity. Because  $e$  is a constant,  $n$  and  $u$  will affect the electric conductivity of the conductor and they have relation to Eg, bond-gap, BW<sub>HO</sub> and BW<sub>LU</sub>. The narrower the energy gap and the wider the energy band, the stronger conductive ability the polymer has. The results are shown in table 9.

We know that HOMO, HOMO<sub>-1</sub>, LUMO and LUMO<sub>+1</sub> are  $\pi$  band by the analyses of energy structure and the frontier molecular orbital ingredient. The phenol ring in quinoline contributes mainly to HOMO and HOMO<sub>-1</sub>, while the pyridine ring forms LUMO and LUMO<sub>+1</sub>. HOMO, HOMO<sub>-1</sub>, HOMO<sub>-2</sub>, LUMO and LUMO<sub>+1</sub> of p-2 all are  $\pi$  band. The frontier occupied orbits are mainly dominated by the substituted group of styryl, and the contribution of the quinoline and styryl is similar, which is consistent with the orbital ingredient analysis. Just for the effect of sub-

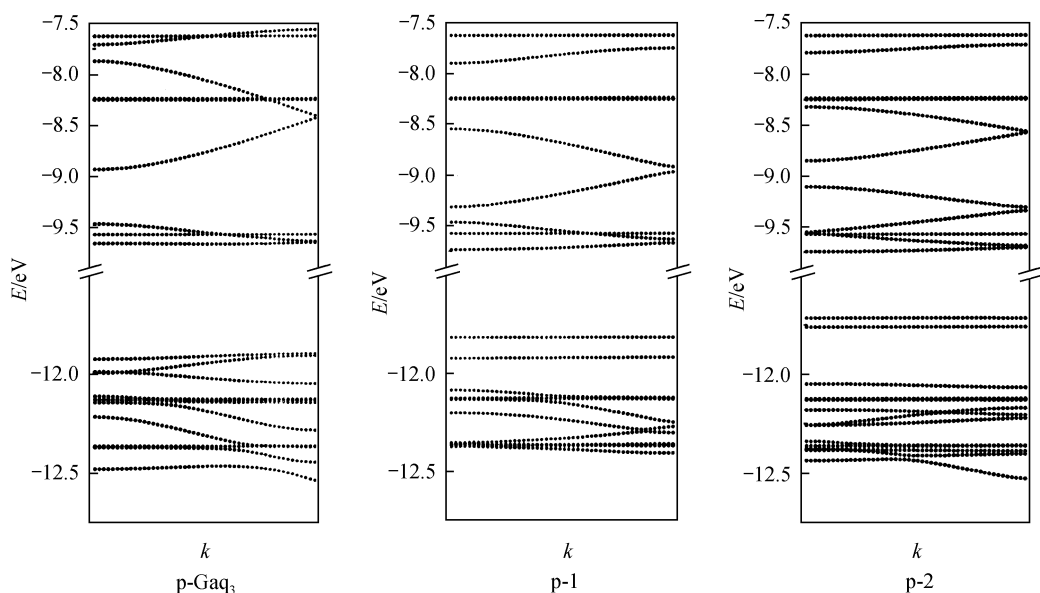


Fig. 4. Energy band structures of  $\text{Gaq}_3$  and its derivatives.

stitute, the bond gap energy decreases, and conductive gap energy increases, which makes the energy gap become less. It reflects further the importance of the substituted group. The derivative of  $\text{Gaq}_3$  will be an ideal luminescence material for it maintains the same property of  $\text{Gaq}_3$  and its embedded one.

Table 9 Energy band parameters of  $\text{Gaq}_3$  and its derivatives/eV

System	p- $\text{Gaq}_3$	p-1	p-2
Eg	2.234 0	2.086 5	1.969 0
BW <sub>HO</sub>	0.028 3	0.000 4	0.001 1
BW <sub>LU</sub>	0.009 2	0.064 8	0.039 0
I <sub>p</sub>	11.923 3	11.817 8	11.713 8
Au	9.661 4	9.731 3	9.744 7

According to the calculation result of EHMO-CO, we find that  $\text{Gaq}_3$  can keep less energy gap and possess good electron-delivered function if it is polymerized. Compared with  $\text{Gaq}_3$ , its derivatives substituted with ethylene and styryl have little energy gap, and they will have better function than  $\text{Gaq}_3$ . It will become a better optical material, because its energy gap becomes more rich, which not only possesses energy characteristics of styryl unit, but also maintains original characteristics of 8-hydroxyquinoline, together with new change in interaction, which is favorable to the adjustment of spectrum wave in optical materials.

## References

1. Tang, C. W., VanSlyke, S. A., Organic electroluminescent diodes, *Appl. Phys. Lett.*, 1987, 51(12): 913.
2. VanSlyke, S. A., Chen, C. H., Tang, C. W., Organic electroluminescent devices with improved stability, *Appl. Phys. Lett.*, 1996, 69: 2160.
3. Hamada, Y., Sano, T., Fujita, M. et al., High luminance in organic electroluminescent devices with bis(10-hydroxybenzo-

- quinolinato)beryllium as an emitter, Chem. Lett., 1993: 905.
4. Kido, J., Ikeda, W., Kimura, M. et al., White-light-emitting organic electroluminescent device using lanthanide complexes, Jpn. J. Appl. Phys., 1996, 35: L394.
  5. Shen, Z., Burrows, P. E., Bulovic, V. et al., Three-color, tunable, organic light-emitting devices, Science, 1997, 276: 2009.
  6. Burrows, P. E., Sapochak, L. S., McCarty, D. M. et al., Metal ion dependent luminescence effects in metal tris-quinolate organic heterojunction light emitting devices, Appl. Phys. Lett., 1994, 64(20): 2718.
  7. Wang, Y., Zhang, W., Li, Y. et al., X-ray crystal structure of gallium tris-(8-hydroxyquinoline): intermolecular  $\pi$ - $\pi$  stacking interactions in the solid state, Chem. Mater., 1999, 11: 530.
  8. Stampor, W., Kalinowski, J., Marco, P. D. et al., Electric field effect on luminescence efficiency in 8-hydroxyquinoline aluminum thin films, Appl. Phys. Lett., 1997, 70: 1935.
  9. Stampor, W., Kalinowski, J., Marconi, G. et al., Electroabsorption study of excited states in tris 8-hydroxyquinoline aluminum complex, Chem. Phys. Lett., 1998, 283: 373.
  10. Higginson, K. A., Zhang, X., Papadimitrakopoulos, F., Thermal and morphological effects on the hydrolytic stability of aluminum tris(8-hydroxyquinoline), Chem. Mater., 1998, 10: 1017.
  11. Xue, W. M., Chan, M. C. W., Su, Z. M. et al., Spectroscopic and excited-state properties of luminescent rhenium(I) N-heterocyclic carbene complexes containing aromatic diimine ligands, Organomet., 1998, 17(8): 1622.
  12. Xue, W. M., Wang, Y., Chan, M. C. W. et al., Tuning the excited-state properties of luminescent rhenium(V) benzyldiene complexes containing phosphorous and nitrogen donor ligands, Organomet., 1998, 17(10): 1946.
  13. Burrows, P. E., Shen, Z., Bulovic, V. et al., Relationship between electroluminescence and current transport in organic heterojunction light-emitting devices, J. Appl. Phys., 1996, 79: 7991.
  14. Frisch, M. J., Trucks, G. W., Schlegel, H. B. et al., Gaussian 94, Revision B.2, Pittsburgh PA: Gaussian, Inc., 1995.
  15. Whangbo, M. H., Evain, M., Hughbanks, T. et al., Extended huckel molecular, crystal and properties package, QCPE571, Indiana Univ, 1987.
  16. Wakimoto, T., Murayama, R., Nagayama, K. et al., Organic EL cells with high luminous efficiency, Appl. Surf. Sci., 1997, 113: 698.
  17. Su, Z. M., Cheng, H., Gao, H. Z. et al., *Ab initio* and DFT study on electronic structures and photoelectric properties of tris 8-hydroxyquinoline aluminum, Chemical J. of Chinese Universities, 2000, 21(9): 1620.
  18. Huang, Z. H., Xie, D. M., Wang, R. S. et al., New type of electro-luminescence material——poly(p-phenylene vinylene), Journal of Functional Materials, 1993, 24: 97.
  19. Wang, R. S., Huang, Z. H., Wang, D. M. et al., The energy-band structure and electric property of PPV and its N-substitutes, Chinese Science Bulletin, 1994, 39(8): 637.
  20. Huang, Z. H., Tong, L. G., Wang, X. J. et al., Studies on preparation of poly(PV-co-DMeOPV) and its characteristic of PL and EL, Chemical J. of Chinese Universities, 1998, 19(12): 2020.
  21. Liu, C. L., Su, Z. M., Feng, J. K. et al., Theoretical studies on non-resonant third-order nonlinear optical properties of symmetrical stilbene derivatives, Acta Chimica Sinica, 2000, 58(2): 184.
  22. Aziz, H., Popovic, Z., Xie, S. et al., Humidity-induced crystallization of tris(8-hydroxyquinoline)aluminum layers in organic light-emitting devices, Appl. Phys. Lett., 1998, 72: 756.